Journal of Solid State Chemistry **149,** 123–132 (2000)
Article ID jssc.1999.8509, available online at http://www.idealibrary.com on IDEAL®

The Phase Transition of TlTe: Crystal Structure

Klaus Stöwe

Institut für Anorganische Chemie und Analytische Chemie und Radiochemie, Universität des Saarlandes, P.O. Box 151150, 66041 Saarbrücken, Saarland, Germany,

Received June 4, 1999; accepted September 21, 1999

Though already known since the year 1912, reliable structural data of the semimetallic phase TlTe down and below the reported phase-transition temperature of 170 K were still lacking. To fill this gap, we performed low-temperature X-ray diffraction investigations on single crystals of TlTe down to 135 K with a conventional laboratory radiation source (Mo$K\alpha$) and additionally at the D3 synchrotron beamline of HASLYLAB at DESY ($\lambda = 40$ pm). The compound TlTe crystallizes at ambient temperature tetragonal in space group $I4/mcm$ and the lattice parameters $a = 1295.3(1)$ pm and $c = 617.3(1)$ pm. The crystal structure reveals univalent Tl^+ cations and a polytelluric counterpart with linear equidistant Te chains in the [001] direction at distances of 308.63(3) pm. One-half of the chains is unbranched; the other one consists of linear [Te_3] units stacked cross-shaped one upon the other. At 172 K one-half of the branched chains transforms by a Peierls distortion into a linear chain with alternating distances of 285.5(1) and 330.2(1) pm. By the transformation the unit cell volume is doubled and the space group changed into $P4_2/nmc$ ($a = 1822.9(1)$ pm and $c = 615.7(1)$ pm at 157 K). Since the other half of the branched chains and the other unbranched chains remain equidistant, it is to be expected that the compound keeps up its semimetallic behavior. This finding is in accordance with experimental resistivity data in the literature. © 2000 Academic Press

INTRODUCTION

Even in 1949 it was known from Debye–Scherrer X-ray diffraction diagrams (1) that TlTe has a crystal structure different from the large number of binary and ternary phases of the TlSe structure type as, e.g., InTe at ambient pressure (2). Instead of crystallizing as mixed valence compound $Tl^+Tl^{3+}(Te^{2-})_2$, it forms polyanionic structure fragments, $Tl^+(Te_n)^-_{1/n}$. The phase TlTe was first reported by Chikashigé (3) in 1912, who studied the binary phase diagram Tl–Te by thermal analysis. The data from this analysis and the analyses of Obukhov *et al.* (4) were the basis for a phase diagram given by Hansen (5), which was revised in 1960 by Rabenau *et al.* (6). The first revision of the crystal structure of TlTe (7) in respect to the tellurium arrangement was published by Weis *et al.* (8) ($R = 0.102$), whereas the reinvestigation of the Tl–Te system by thermal analysis and X-ray diffraction by Toure *et al.* (9) revealed no further changes of the structure model of TlTe ($R = 0.059$). The electrical properties of TlTe were measured by Jensen *et al.* (10) in 1972. Resistivity and Hall-coefficient data suggested TlTe to be semimetallic and to have a phase transition at 170 K with a resistivity hump by a factor of 2–3. But these data are rather unsatisfying since, on one hand, the samples have shown the presence of additional phases as indicated by the occurrence of extra thermal effects in the differential thermal analysis data, and on the other hand, there were some absurdities in (10) between the composition and physical properties. Hence, reliable low-temperature resistivity data are still lacking, which would give a clue as to whether TlTe is a superconductor.

The intention of our own investigations was the examination of the reported phase transition at 170 K by X-ray diffraction methods to get reliable information on the structural changes at the transition temperature. By this, the data of the former investigations concerning the room-temperature polymorph were further improved ($R_w = 0.017–0.021$, reduced ESDS). Additionally, a hitherto unknown low-temperature polymorph was found and characterized by single-crystal X-ray diffraction experiments.

EXPERIMENTAL

Sample Synthesis

According to the phase diagram of Rabenau *et al.* (6), TlTe is incongruently melting at 300°C. For that reason crystals of TlTe were obtained from the elements Tl (rod, 99.999%, Chempur, Karlsruhe, Germany) and Te (pieces, >99.999%, Fluka, Buchs, Switzerland) by homogenizing samples of a composition of 60 mol% tellurium in sealed Pyrex ampoules at 450°C and subsequently cooling from 300 to 240°C at a rate of 0.2°C/h. Needle-shaped single crystals of TlTe formed at the surface of the solidified regulus, which could readily be dissected.

0022-4596/00 $35.00
Copyright © 2000 by Academic Press
All rights of reproduction in any form reserved.

TABLE 1
***P*4 Measurement Data of Thallium Telluride in the X-Ray Single-Crystal Structure Analysis (in Brackets at 157 K)**

Chemical formula	TlTe
Molecular weight	331.98 g mol^{-1}
Crystal size	$0.09 \times 0.13 \times 0.32$ mm^3
Color	Lustrous metallic
Number of formula units per cell	16 (32)
Space group	*I*4/*mcm*/No. 140 (*P*4$_2$/*nmc*/No. 137)
Diffractometer type	SIEMENS P4
Measured range of reciprocal space (Mo$K\alpha$)	$3 < 2\theta < 60^\circ$ (all octants)
Monochromator	Plan HOPG crystal
Scan type/range	$\omega/0.8^\circ$ ($\omega/0.8^\circ$) in 96 steps
Scan speed	Variable, 2–5° min^{-1} (2.5–7.5° min^{-1})
Absorption correction	Numerical[a,b]
Structure solution	Direct methods (transformed data)
Structure refinement	Full-matrix least-squares
Program for structure solution and refinement	SHELXTL PLUS[c]
Extinction parameter	Empirical with $F^* = F[1 + 0.002\,\chi F^2/\sin(2\theta)]^{-1/4}$
Number of independent parameters	17(44)

[a]W. Herrendorf, "HABITUS, Program for the Optimization of the Crystal Description for a Numerical Absorption Correction on the Basis of Appropriate Psi-Scanned Reflections." Karlsruhe, Germany, 1992.

[b]N. W. Alcock, P. J. Marks, and K.-G. Adams, "ABSPSI, Absorption Correction and Refinement of the Crystal Habitus." Karlsruhe, Germany, 1994.

[c]"SHELXTL PLUS, V.4.0, Program for Determination of Crystal Structures with X-Ray and Neutron Data." Siemens Analytical X-Ray Instruments, Inc., Madison WI, 1990.

X-Ray Crystal Structure Determination and Refinement

Data collections were carried out with a P4-type single-crystal diffractometer (Siemens, Karlsruhe, Germany) and the structure refinement with the program SHELXTL (11). For low-temperature measurements the diffractometer was equipped with a Siemens LT-2A low-temperature attachment. Details concerning the instrument and the refinement procedure are already given in (12). To get information about the low-temperature superstructure, additional measurements at the D3 synchrotron beamline of HASYLAB at DESY in Hamburg, Germany were performed using a Huber 4-circle diffractometer with a large offset Eulerian cradle of 400 mm inner diameter and an Oxford Cryo-Systems cooling attachment. Intensities were collected with a fast plastic scintillation counter at a wavelength of $\lambda = 40$ pm. Tables 1–7 give summaries of important measurement and refinement data including the refined parameters and Tables 8 and 9 give selected interatomic distances below 400 pm.

CRYSTAL STRUCTURE

Considering the different positional parameters of TlTe in the room-temperature polymorph (see Table 5), it becomes immediately clear that the compound contains monovalent thallium ions instead of mixed valent cations as in compounds of the TlSe structure type. These are surrounded by seven tellurium ions in a $4 + 3$ manner as shown in Fig. 1. The shortest Tl–Tl distance is 350.2 pm (at ambient temperature, see Table 8). This distance separates two thallium ions in adjacent coordination polyhedra connected by a common quadrangular face Te(1)–Te(1)–Te(1)–Te(2). The next nearest two Tl cations are 371.2 pm apart. All these distances are far beyond typical covalent Tl^{2+}–Tl^{2+} interactions, despite the fact that there is reported an enormous spread of Tl–Tl bonding distances in the literature. In the Tl_2^{4+} fragment of the compound $Tl_{0.8}Sn_{0.6}Mo_7O_{11}$, the Tl cations are 284.0(3) pm apart (13), whereas in the molecular compounds $[H_3CC(CH_2NSiMe_3)_3Tl_2]_2$, $[(Me_3Si)_3Si]_4Tl_2$, and $(tBu_3Si)_4Tl_2$ Tl–Tl distances of 273.4(2) pm (14), 291.42(5) pm (15), and 296.6(2) pm (16) are observed, respectively. At the HF-SCF level in the compound D_{2d}–Tl_2H_4

TABLE 2
D3 Synchrotron Beamline Measurement Data of Thallium Telluride at 157 K

Chemical formula	TlTe
Molecular weight	331.98 g mol^{-1}
Crystal size	$0.09 \times 0.13 \times 0.32$ mm^3
Color	Lustrous metallic
Number of formula units per cell	32
Space group	*P*4$_2$/*nmc*/No. 137
Diffractometer type	Huber 4-circle diffractometer
Wavelength	39.91 pm
Measured range of reciprocal space	$1.5 < 2\theta < 33^\circ$ (2 octants)
Monochromator	Fixed-exit double-crystal type, Flat Si(111) crystal
Detector aperture	3.0×3.0 mm^2
Scan type/range	$\omega/0.615^\circ$ in 41 steps With prescan $\omega/0.525^\circ$ in 15 steps
Scan speed	Variable, 0.1–1 s/step
Drift correction of standard reflections	[a]
Absorption correction	Numerical[b]
Structure solution	Transformed RT data
Structure refinement	Full-matrix least-squares
Program for structure solution and refinement	SHELXTL PLUS[c]
Extinction parameter	Empirical with $F^* = F[1 + 0.002\,\chi F^2/\sin(2\theta)]^{-1/4}$
Number of independent parameters	45

[a]K. Eichhorn, "AVSORT Program," unpublished.

[b]K. Eichhorn, "ABSCOR Program," unpublished.

[c]"SHELXTL PLUS, V.4.0, Program for Determination of Crystal Structures with X-Ray and Neutron Data." Siemens Analytical X-Ray Instruments, Inc., Madison, WI, 1990.

TABLE 3
Lattice Parameters from the Single-Crystal Data Refinement in the Temperature Interval 297–135 K

T (K)	a (pm)	c (pm)
293	1295.3(1)	617.3(1)
244	1292.7(1)	616.4(1)
214	1291.2(1)	615.9(1)
199	1290.6(1)	615.7(1)
184	1290.0(1)	615.6(1)
177	1289.8(1)	615.4(1)
175	1289.7(1)	615.4(1)
173	1289.6(1)	615.6(1)
171	1290.0(1)	615.4(1)
169	1290.2(1)	615.7(1)
167	1290.3(1)	615.6(1)
165	1290.2(1)	615.7(1)
163	1290.2(1)	615.6(1)
161	1290.2(1)	615.7(1)
159	1290.2(1)	615.6(1)
157	1290.2(1)	615.7(1)
146	1289.8(1)	615.6(1)
135	1289.5(1)	615.5(1)

a Tl–Tl distance of 277.5 pm was calculated (16). On the other hand, the situation of neighboring Tl ions in polyhedra sharing common faces is typical for compounds with ns^2-configurated Tl^+ or In^+ ions like, e.g., Tl_3SnI_5 or In_3SnI_5. Different from TlTe, in the two mentioned compounds the lone pair cations are surrounded in a 2-fold capped trigonal prismatic manner. The shortest intercationic distances are 371.2(4) pm (18) and 345.4–347.4 pm (19), respectively. Uncommon interactions between metal ions with formally d^{10} or $d^{10}s^2$ configuration were the subject of systematic investigations in the last decade (20, 21). Even for compounds of the univalent metals of group 13, aggregations especially by weak attractive M–M interactions are to be expected. So despite distinct differences in the coordination number, from a crystal chemical point of view, we have to assume Tl^+ ions in TlTe, too. According to common bonding concepts (Zintl–Klemm concept and Moser–Pearson equation), additional polytelluric structure fragments are to be observed in TlTe. In fact, these are found as linear equidistant Te(3) chains along the direction [001] with distances of d(Te(3)–Te(3)) = 308.6 pm and branched chains of Te(1) and Te(2). In the latter ones [Te(1)–Te(2)–Te(1)] units are stacked cross-shaped one upon the other along [001] with distances of d(Te(1)–Te(2)) = 301.5 pm within the [Te_3] unit and d(Te(2)–Te(2)) = 308.6 pm from unit to unit. These are depicted in Fig. 2, which shows the crystal structure of TlTe in the form of discrete ions and polytelluric structure fragments (left side), and in the form of a polyhedral description (right side). All other Te–Te distances are lying well above 430 pm and indicate that there are no further homonuclear interactions in TlTe ($r(Te^{2-}) = 220$ pm). For the discussion of the bonding characteristics as reference length for a covalent single Te–Te bond the compound Ph_2Te_2 may serve in which the tellurium atoms are 271 pm apart (22). With 301 and 308.6 pm the covalent Te–Te bonding distances in TlTe are in the same range as those in several other polytelluric compounds with linear Te anion arrangements, e.g., UTe_2 (305.7(1) and 307.6(1) pm (12) or U_2Te_5 (290.3(1), 303.3(1), 304.7(1), and 317.7(1) pm (23)). Inspecting a (110) section of the crystal structure of TlTe reveals that the arrangement of $^1_\infty$[Te_3] units stacked cross-shaped to chains in the [001] direction can be regarded as a fragmentation pattern of a regular 4^4 net. This is depicted in Fig. 3. Topologically, the arrangement of Te(1)/(2) in TlTe is observed from the 4^4 net by braking bonds every third linear row to the neighboring row in one direction of the plane and rotating every second linear [Te_3] unit about a perpendicular axis out of the net plane by 90°. An explanation for this fragmentation of a regular 4^4 net will be given in a following paper (see subsequent contribution: Electronic Bandstructure Calculations).

Resistivity measurements revealed TlTe to show a phase transition at 170 K, but the nature of the transition was

TABLE 4
***P*4 Refinement Data of Thallium Telluride as a Function of Temperature**

Temperature (K)	293	244	214	184	157
Lattice parameters (pm)					
a	1295.3(1)	1292.7(1)	1291.2(1)	1290.0(1)	1290.2(1)
c	617.3(1)	616.4(1)	615.9(1)	615.6(1)	615.7(1)
Calculated density (g cm^{-3})	8.52	8.56	8.59	8.61	8.61
Linear absorption coeff. (mm^{-1})	72.99	73.41	73.64	73.81	73.78
No. of observed reflections	6092	5915	5885	5876	5871
No. of nonequiv. reflections	473	468	466	466	466
Internal R value[a]	6.94	7.20	7.28	7.13	7.38
Extinction parameter	0.0027(1)	0.0026(1)	0.0024(1)	0.0020(1)	0.0021(1)
R value	0.0236	0.0212	0.0196	0.0192	0.0226
R_w value ($w = 1/\sigma(F_o)^2$)	0.0208	0.0190	0.0170	0.0171	0.0197

[a]K.-G. Adams, "MITTELN, Averaging Symmetry-Equivalent Reflections." Karlsruhe, Germany, 1995.

TABLE 5
Positional Parameters and Displacement Factor[a] of the Compound TlTe in *I*4/*mcm* as a Function of Temperature

	Atom	Wyck.	Symm.	Position
	Tl	16*k*	*m*..	$x\ y\ 0$
	Te(1)	8*h*	*m*.2*m*	$x\ x+\frac{1}{2}\ 0$
	Te(2)	4*d*	*m*.*mm*	$0\ \frac{1}{2}\ 0$
	Te(3)	4*a*	422	$0\ 0\ \frac{1}{4}$

	Temperature (K)				
	293	244	214	184	157
Tl					
x	0.07960(3)	0.07948(2)	0.07945(2)	0.07940(2)	0.07953(2)
y	0.22922(3)	0.22932(3)	0.22932(2)	0.22936(2)	0.22913(3)
U_{11}	312(2)	259(2)	218(2)	191(2)	176(2)
U_{22}	369(2)	308(2)	262(2)	231(2)	211(2)
U_{33}	454(3)	377(2)	328(2)	293(2)	280(2)
U_{12}	−13(1)	−8(1)	−7(1)	−4(1)	−4(1)
Te(1)					
x	0.16458(4)	0.16472(4)	0.16482(3)	0.16485(3)	0.16450(4)
U_{11}	262(3)	219(2)	183(2)	158(2)	143(2)
U_{33}	377(5)	320(4)	277(3)	251(4)	350(5)
U_{12}	87(3)	70(3)	62(2)	52(2)	43(3)
Te(2)					
U_{11}	227(3)	189(3)	156(2)	137(2)	134(3)
U_{33}	253(5)	219(5)	197(4)	179(4)	222(5)
U_{12}	56(4)	43(3)	38(3)	30(3)	30(3)
Te(3)					
U_{11}	291(3)	238(3)	201(3)	175(3)	198(3)
U_{33}	281(6)	237(5)	219(5)	212(5)	202(6)

[a] U_{ij} values are given in pm^2. The dimensions are in accordance with the following formula: $-2\pi^2 \sum_i \sum_j U_{ij} h_i h_j a_i^* a_j^*$.

unknown. So we performed X-ray structural investigations as a function of temperature down to 135 K on single-crystal specimens (Fig. 4). On cooling down from room temperature, the lattice parameters *a* and *c* of the tetragonal unit cell revealed a sudden hump. Beginning at 171–173 K, both the *a* and *c* axis start to expand and reach a maximum at 167–169 K. The volume increase at the transition from 173 to 167 K is about 0.15%, relatively small. At several discrete temperatures a complete data set was collected and the structural parameters were refined (see Tables 4 and 5). From room temperature down to 184 K the refined positional parameters *x*(Te(1)), *x*(Tl), and *y*(Tl) vary almost linearly with temperature: *x*(Te(1)) and *y*(Tl) increase with temperature on cooling down, whereas *x*(Tl) decreases. Beyond the independent displacement parameters U_{11} and U_{33} of Te(1/2/3) show a linear decreasing relationship on the temperature lowering. In Tables 4 and 5 and Figs. 5 and 6 also the corresponding parameters at 157 K below the phase-transition temperature due to a refinement in the same structure model as above are given and several anomalies in the positional as well as the displacement parameters are observed. But image plate rotation photographs about the three direct crystal axes at 150 K at the D3

TABLE 6
Refinement Data of Thallium Telluride in $P4_2/nmc$ at 157 K

Diffractometer	Siemens *P*4	Huber (D3)
Lattice parameters (pm)		
a	1822.9(1) pm	[a]
c	615.7(1) pm	
Calculated density (g cm^{-3})	8.62	8.62
Linear absorption coeff. (mm^{-1})	73.92	14.68
No. of observed reflections	23749	8541
No. of nonequiv. reflections	1582	1641
Internal *R* value[b]	0.1090	0.0609
Extinction parameter	0.00006(1)	0.00004(1)
R value	0.0576	0.0349
R_w value ($w = 1/\sigma(F_o)^2$)	0.0429	0.0372

[a] Wavelength calibrated to fit cell parameters of Siemens *P*4 data.

[b] K.-G. Adams, "MITTELN, Averaging Symmetry-Equivalent Reflections." Karlsruhe, Germany, 1995.

TABLE 7

Positional Parameters and Displacement Factor[a] of the Compound TlTe in $P4_2/nmc$ at 157 K (For the Purpose of Comparison Positional Parameters in LT Setting Transformed from Data at 157 K Refined in the RT Structure Model Are Also Given (Last Column))

Atom	Wyck.	Symm.	Position
Tl(a)	16*h*	1	*x y z*
Tl(b)	16*h*	1	*x y z*
Te(1a)	8*g*	.*m*.	$\frac{1}{4}$ *y z*
Te(1b)	8*g*	.*m*.	$\frac{1}{4}$ *y z*
Te(2a)	4*d*	2*mm*.	$\frac{1}{4}$ $\frac{1}{4}$ *z*
Te(2b)	4*c*	2*mm*.	$\frac{3}{4}$ $\frac{1}{4}$ *z*
Te(3)	8*f*	..2	*x x* $\frac{1}{4}$

Diffractometer	Siemens *P*4	Huber (D3)	Transformed
Tl(a)			
x	0.07500(5)	0.07484(1)	0.07480
y	0.84593(5)	0.84562(1)	0.84567
z	0.5077(1)	0.50779(2)	0.5
U_{11}	174(4)	179(1)	
U_{22}	179(4)	175(1)	
U_{33}	249(5)	215(1)	
U_{23}	−3(3)	−2(1)	
U_{13}	−5(3)	−1(1)	
U_{12}	−15(3)	−16(1)	
Tl(b)			
x	0.15462(5)	0.15420(1)	0.15433
y	0.07454(5)	0.07468(1)	0.07480
z	0.5055(1)	0.50522(2)	0.5
U_{11}	180(4)	166(1)	
U_{22}	200(4)	177(1)	
U_{33}	289(5)	219(1)	
U_{23}	−0(3)	−3(1)	
U_{13}	−2(3)	0(1)	
U_{12}	−21(3)	−18(1)	
Te(1a)			
y	0.4145(1)	0.41461(3)	0.4145
z	0.0046(3)	0.00487(5)	0.0
U_{11}	186(10)	207(3)	
U_{22}	117(9)	125(3)	
U_{33}	290(11)	310(3)	
U_{23}	−3(6)	0(1)	
Te(1b)			
y	0.9145(1)	0.91440(3)	0.9145
z	0.4767(3)	0.47718(7)	0.5
U_{11}	161(9)	187(2)	
U_{22}	77(8)	105(2)	
U_{33}	182(8)	151(2)	
U_{23}	13(5)	5(1)	
Te(2a)			
z	0.0032(4)	0.00286(7)	0.0
U_{11}	99(11)	132(4)	
U_{22}	117(12)	185(4)	
U_{33}	194(13)	219(4)	
Te(2b)			
z	0.0193(4)	0.01816(7)	0.0
U_{11}	185(13)	168(3)	
U_{22}	90(11)	111(3)	
U_{33}	107(10)	93(3)	
Te(3)			
x	0.49673(6)	0.49707(1)	0.5
U_{11}	150(3)	176(2)	
U_{33}	215(6)	194(2)	
U_{23}	0(4)	1(1)	
U_{12}	−20(9)	29(2)	

[a] U_{ij} values are given in pm^2. The dimensions are in accordance with the following formula: $-2\pi^2 \sum_i \sum_j U_{ij} h_i h_j a_i^* a_j^*$.

beamline of DESY in Hamburg revealed superstructure reflections corresponding to a doubling of both the tetragonal a_1 and a_2 axes. Due to a change of Bravais type from *I* to *C* the new unit cell was transformed into a conventional *P*-type setting with cell parameters given in Table 6. The new *P*-type cell has a 2-fold volume compared to the original one and hence contains twice as many formula units. According to group–subgroup relations, there are eight different possible *C*-centered subgroups of $I4/mcm$ with a doubling of the unit cell in both directions of the tetragonal basis. These are to be derived from the maximal nonisomorphic subgroup $P4/mcc$ and $P4_2/mcm$. Extinction conditions reduce these possibilities to a single space group, $C4_2/acm$ or, in a conventional setting, $P4_2/nmc$. In the conventional *P*-type setting the reflection conditions are $hk0$, $h + k = 2n$; hhl, $l = 2n$; and $h00$, $h = 2n$. Since both

TABLE 8

Selected Interatomic Distances in RT Polymorph of TlTe below 400 pm (in pm, see also Fig. 8)

Temperature (K)	293	244	214	184	157
Tl–Te(1)	341.77(7)	341.04(6)	340.54(5)	340.26(5)	340.63(6)
Tl–Te(1)	344.90(7)	344.10(6)	343.75(5)	343.38(5)	343.47(6)
Tl–Te(3) 2×	350.14(4)	349.53(4)	349.15(3)	348.89(3)	348.74(4)
Tl–Te(1) 2×	355.38(4)	354.80(4)	354.48(4)	354.30(4)	354.43(5)
Tl–Te(2)	365.57(5)	364.67(4)	364.25(3)	363.85(3)	364.24(5)
Tl–Tl	350.20(8)	349.53(7)	349.19(5)	348.90(5)	349.13(7)
Tl–Tl 2×	371.18(5)	370.41(4)	370.03(4)	369.76(4)	369.97(4)
Te(1)–Te(2)	301.48(5)	301.12(5)	300.97(4)	300.75(4)	300.16(5)
Te(2)–Te(2)	308.63(3)	308.20(3)	307.93(4)	307.82(3)	307.83(4)
Te(3)–Te(3)	308.63(3)	308.20(3)	307.93(4)	307.82(3)	307.83(4)
S[a]	113.4	111.5	111.0	110.3	113.3

[a] Calculated as Tl displacement from the center of gravity of the tellurium coordination polyhedron

TABLE 9
Selected Interatomic Distances and Angles in LT Polymorph of TlTe below 400 pm (in pm)

Diffractometer	Siemens *P*4	Huber (D3)
Tl(a)–Te(1a)	341.0(2)	340.24(5)
Tl(a)–Te(1b)	343.2(1)	343.56(3)
Tl(a)–Te(3)	343.3(1)	344.39(3)
Tl(a)–Te(1b)	346.3(2)	346.32(5)
Tl(a)–Te(3)	353.4(1)	352.95(3)
Tl(a)–Te(1b)	363.0(2)	362.40(5)
Tl(a)–Te(2b)	363.9(1)	363.84(3)
Tl(b)–Te(1b)	340.1(2)	340.83(5)
Tl(b)–Te(1a)	343.8(1)	343.33(3)
Tl(b)–Te(3)	347.8(1)	347.50(3)
Tl(b)–Te(3)	349.9(1)	349.10(3)
Tl(b)–Te(1a)	353.7(2)	354.30(4)
Tl(b)–Te(1a)	354.6(2)	354.68(4)
Tl(b)–Te(2a)	364.1(1)	364.20(3)
Tl(a)–Tl(1a)	349.8(2)	348.62(4)
Tl(a)–Tl(1a)	361.4(2)	361.96(4)
Tl(a)–Tl(1a)	377.2(2)	377.93(4)
Tl(b)–Tl(b)	347.7(2)	349.28(4)
Tl(b)–Tl(b) 2×	370.7(1)	369.88(4)
Te(1a)–Te(2a)	299.8(2)	300.08(6)
Te(2a)–Te(2a) 2×	307.9(1)	307.87(3)
Te(1b)–Te(2b)	301.0(2)	300.75(6)
Te(2b)–Te(2b)	284.1(4)	285.5(1)
Te(2b)–Te(2b)	331.7(4)	330.2(1)
Te(3)–Te(3) 2×	308.3(1)	308.24(4)
S[a]–Tl(a)	111.4	113.8
S–Tl(b)	119.6	117.2
Te(1a)–Te(2a)–Te(2a)	89.84(5)°	89.76(1)°
Te(1b)–Te(2b)–Te(2b)	95.00(5)°	94.81(1)°
Te(3)–Te(3)–Te(3)	173.7(1)°	174.38(1)°

[a]See footnote in Table 8.

symmetry reduction steps, from $I4/mcm$ to $P4_2/mcm$ and further on from $P4_2/mcm$ to $P4_2/nmc$, are *klassengleich* (see Fig. 7), the structural transition in TlTe is not accompanied by the formation of twins. The existence of a symmetry relation shows that there also has to be a close structural correspondence between room and low-temperature polymorphs. To get a starting model for structure refinement, the positional parameters of the room-temperature polymorph were transformed by the matrices given in Fig. 7. Due to the symmetry reduction, several atomic sites split up[1] and the possibility for a differentiation of the various chemical environments opens up. Due to the occurrence of two independent Tl sites in the LT phase, a transition from univalent to mixed valent Tl ions comes within the range of possibility. But as the comparison of the transformed positional parameters of the LT phase at 157 K refined in the RT structure model with the ones refined in space group $P4_2/nmc$ demonstrates (see Table 7), major changes are observed only in the z coordinates of Te(1b) and Te(2b). On the other hand, the cations nearly keep their positions in the RT phase, and the different mean interatomic Tl–Te distances remain almost equal (see also Fig. 8). In the LT polymorph, half of the branched, linear equidistant Te(2) chains has transformed in a Peierls distortion into a chain of Te ions with alternating distances of 285.5(1) and 330.2(1) pm (D3 data, see Table 9), whereas the distances to the neighboring Te(1) ions remain almost constant (d(Te(1b)–Te(2b)) = 300.8(1) pm; see Table 9). The shorter chain distance is comparable to the shortest interatomic distance in elementary tellurium with 283.4 pm (24); the longer one is in the range of secondary interactions. By this, the $^1_\infty[Te_3]$ chains, i.e., $[Te_3]$ units equidistantly stacked cross-shaped one upon the other, fall into an arrangement of discrete $[Te_6]$ units with bended Te(1) ions ($\sphericalangle$(Te(1b)–Te(2b)–Te(2b)) = 94.81(1)°; see Table 9). The other half of Te(1) and Te(2) ions remains almost unchanged, i.e., the linear chain equidistant with an interatomic distance of d(Te(2a)–Te(2a)) = 307.9(1) pm. Apart from linear Te(2) chains, also linear equidistant Te(3) chains are present in

[1]For a close correspondence to the RT polymorph the labels for the different atoms were retained in the LT polymorph and those for split-up sites were extended by an additional labelling as "a" and "b".

TABLE 10
Summary of Compounds with Linear Chalcogen Chains as Structural Fragments (The Distances Given Are Calculated from Single-Crystal Data (sc, Semiconductor; m, Metal)

Compound	d_1 (pm)	d_2 (pm)	d_2/d_1	Conductivity
ZrS_3[a]	208.8	303.6	1.45	sc
NbS_3[b]	205.0	291.4	1.42	sc
USe_3[c]	236.1	329.4	1.40	sc
$ZrSe_3$[a]	234.4	306.8	1.31	sc
UTe_3[d]	275.1	335.0	1.22	sc
TlTe[e]	285.5	330.2	1.16	m
$ZrTe_3$[f]	279.2	310.4	1.11	m
U_2Te_5:U(1)[g]	290.3	317.7	1.09	m
UTe_2 (RT)[h]	305.7	307.6	1.01	m
U_2Te_5:U(2)[f]	303.3	304.7	1.00	m
TlTe[i]	308.5	308.5	1.00	m

[a]S. Furuseth, L. Brattås, and A. Kjekhus, *Acta Chem. Scand. A* **29,** 623 (1995).
[b]J. Rijnsdorp and F. Jellinek, *J. Solid State Chem.* **25,** 325 (1978).
[c]A. Ben Salem, A. Meerschaut, and J. Rouxel, *C. R. Acad. Sci. Paris. Sér. II* **299,** 617 (1984).
[d]K. Stöwe, *Z. Anorg. Allg. Chem.* **622,** 1419 (1996).
[e]This work (see Table 10).
[f]S. Furuseth and H. Fjellvåg, *Acta Chem. Scand.* **45,** 694 (1991).
[g]K. Stöwe, *Z. Anorg. Allg. Chem.* **622,** 1423 (1996).
[h]K. Stöwe, *J. Solid State Chem.* **127,** 202 (1996).
[i]A. A. Toure, G. Kra, R. Eholie, J. Olivier-Fourcade, and J.-C. Jumas, *J. Solid State Chem.* **87,** 229 (1990).

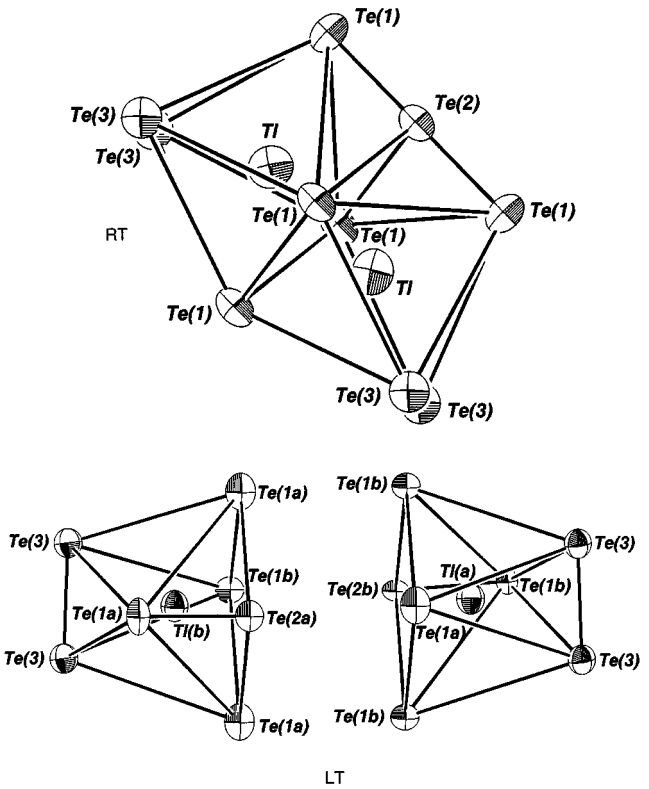

FIG. 1. Coordination polyhedra of the Tl ions in TlTe (ORTEP plot with 95% probability ellipsoids). Top: two equivalent polyhedra of the RT phase connected by a common quadrangular face. Bottom: comparison to the two Tl polyhedra in the LT polymorph.

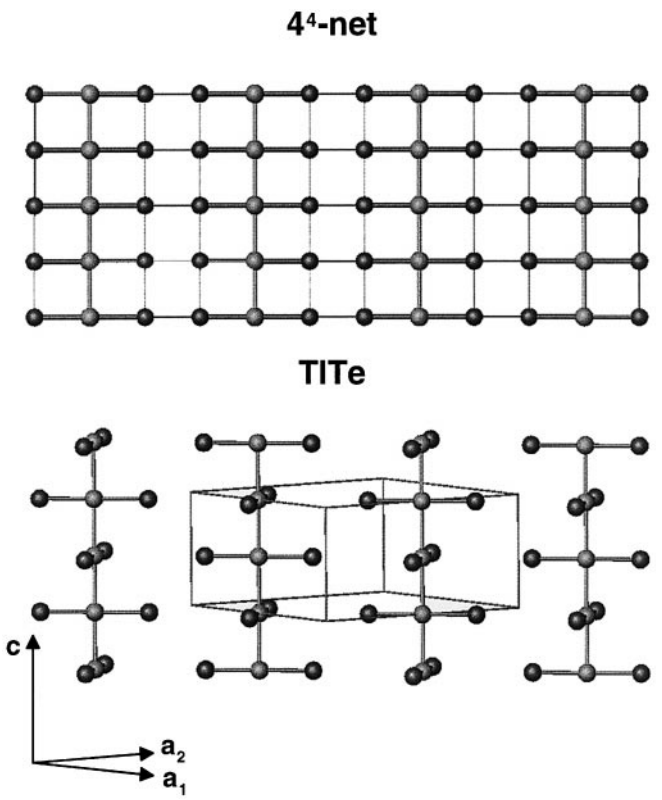

FIG. 3. (110) section through the crystal structure of TlTe. Top: regular 4^4 net. Bottom: fragmentation into chains of $[Te_3]$ units as in TlTe.

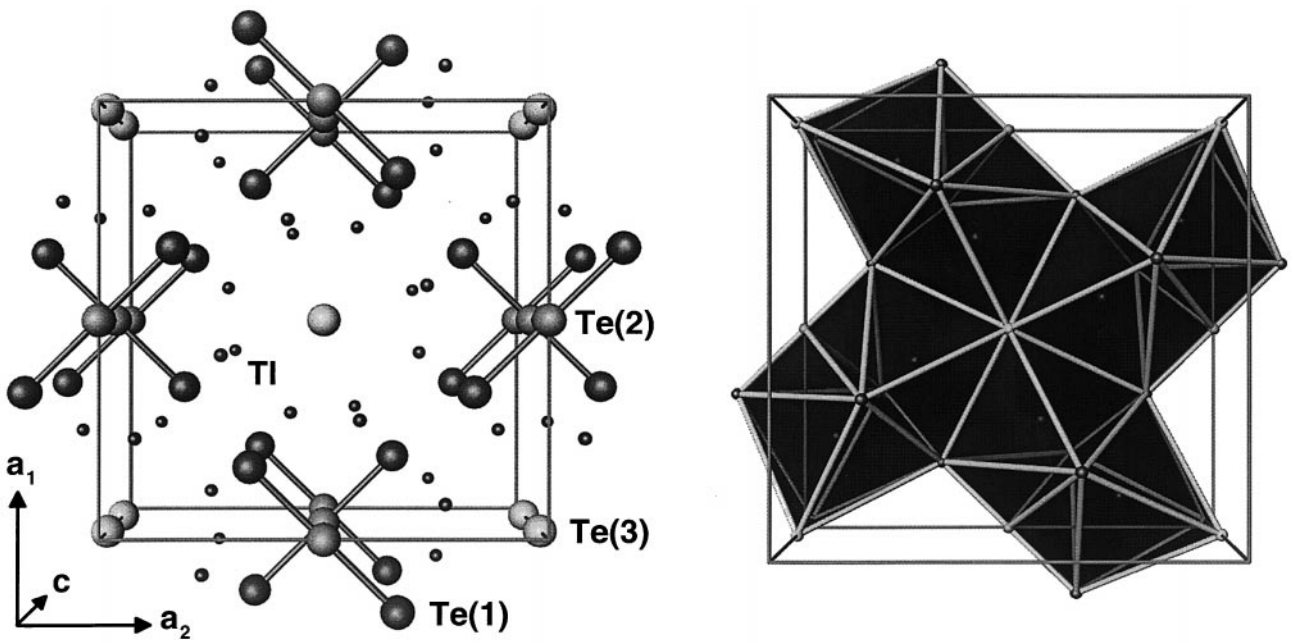

FIG. 2. Crystal structure of RT TlTe along the [001] direction.

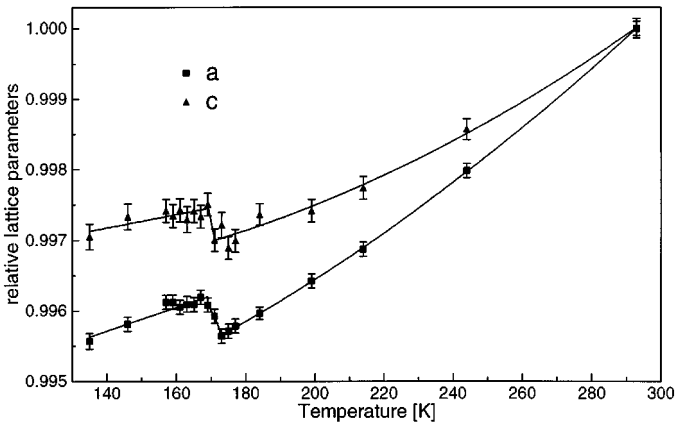

FIG. 4. Relative lattice parameters *a* and *c* of the tetragonal unit cell of TlTe as a function of temperature from X-ray single-crystal investigations.

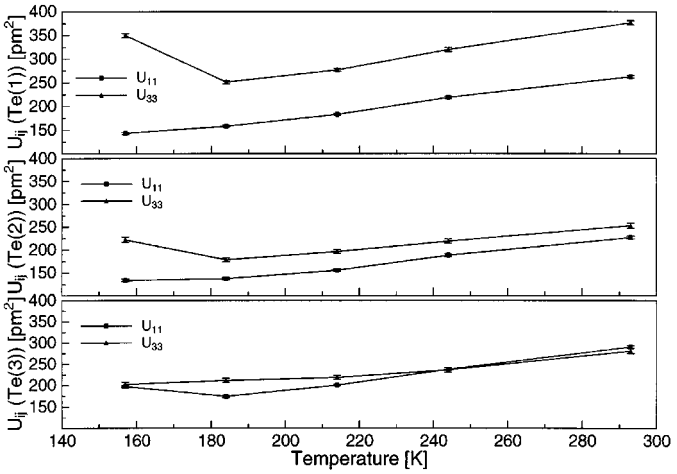

FIG. 6. Independent displacement parameters of TlTe as a function of temperature from single-crystal investigations.

the RT polymorph at crystallographic sites of equal multiplicity. This second type of linear chains remains also equidistant, but the interatomic angles of the Te(3) ions within the chain changes by a few degrees from an exactly linear one to a slightly angled one (∢(Te(3)–Te(3)–Te(3)) = 174.4°). In Fig. 9 projections of the crystal structures are depicted, from which the structural changes occurring during the transition can readily be taken.

DISCUSSION

With the term Peierls distortion we automatically associate a polycationic arrangement. The very intensely studied semiconducting compound VO_2 which undergoes a phase transition at $T_T = 340$ K upon being heated from a structure consisting of $[V_2]$ groups to a metallic form of a tetragonal rutile structure with uniform interaction distances may serve as a typical example. In polyanionic arrangements in some cases distorted linear chains with alternating distances are found. The compounds in Table 10 may serve as examples. From their interatomic distances within the

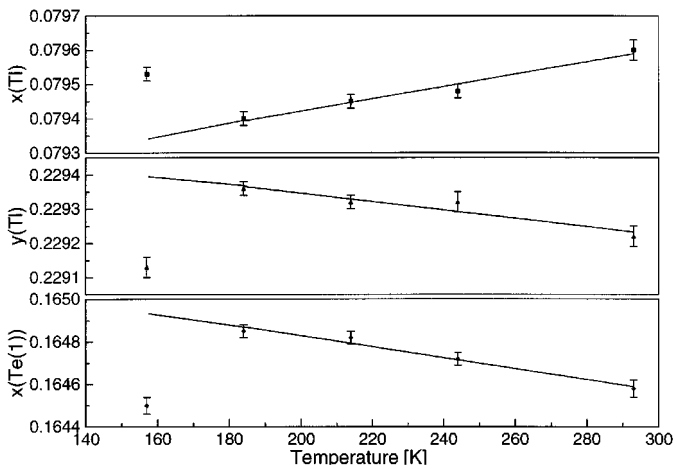

FIG. 5. Independent positional parameters of TlTe as a function of temperature from single-crystal investigations.

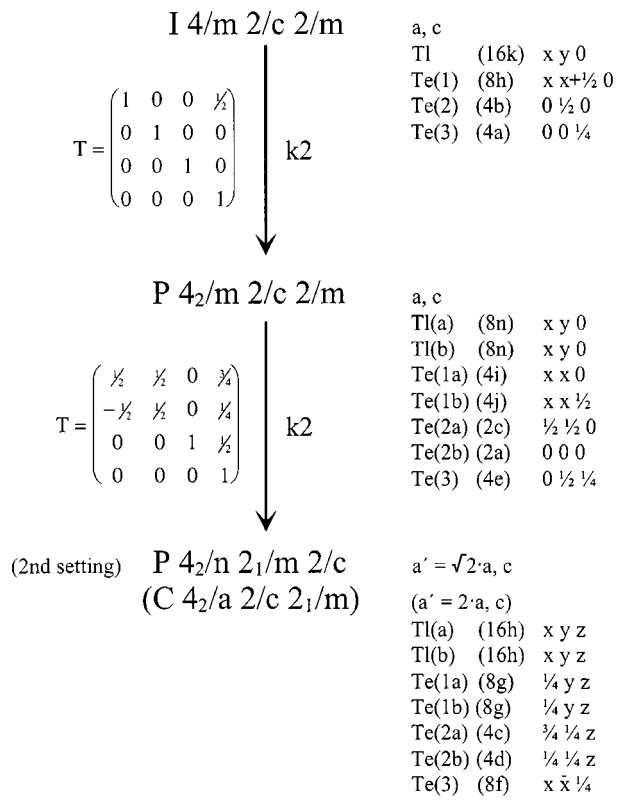

FIG. 7. Group–subgroup relationship between room- and low-temperature polymorphs of TlTe.

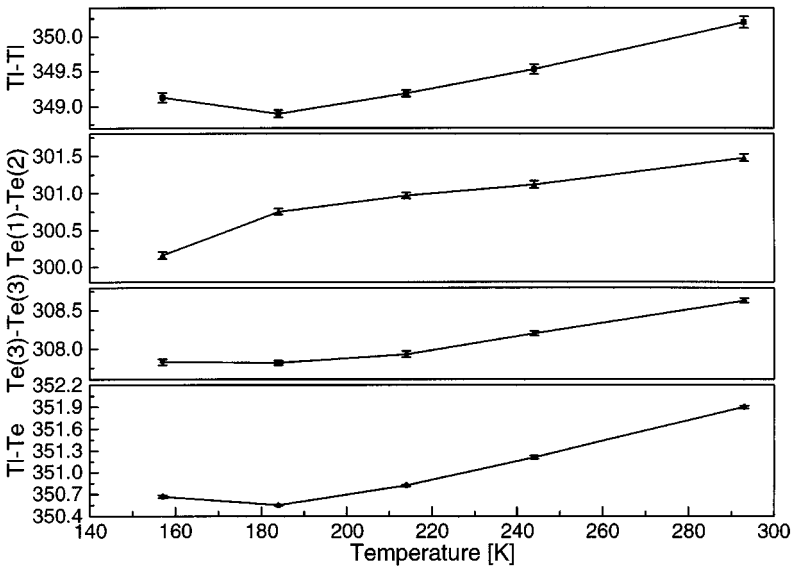

FIG. 8. Selected interatomic distances in TlTe as a function of temperature.

chains, an "alternation" was calculated, which is defined simply as the ratio of the longer (d_2) to the shorter interchain distance (d_1). This ratio varies significantly and all intermediate stages between discrete dumbbells and equidistant chains are observed. But with the exception of TlTe, not one of these compounds shows a phase transition from alternating to equidistant interchain distances at higher temperatures, as far as those actually investigated. Despite distinct alternations, several of these compounds are metallic or semimetallic. Since in TlTe only half of the Te(2) chains is concerned with the phase transition, it is to be expected that the compound keeps up its semimetallic character. Indeed,

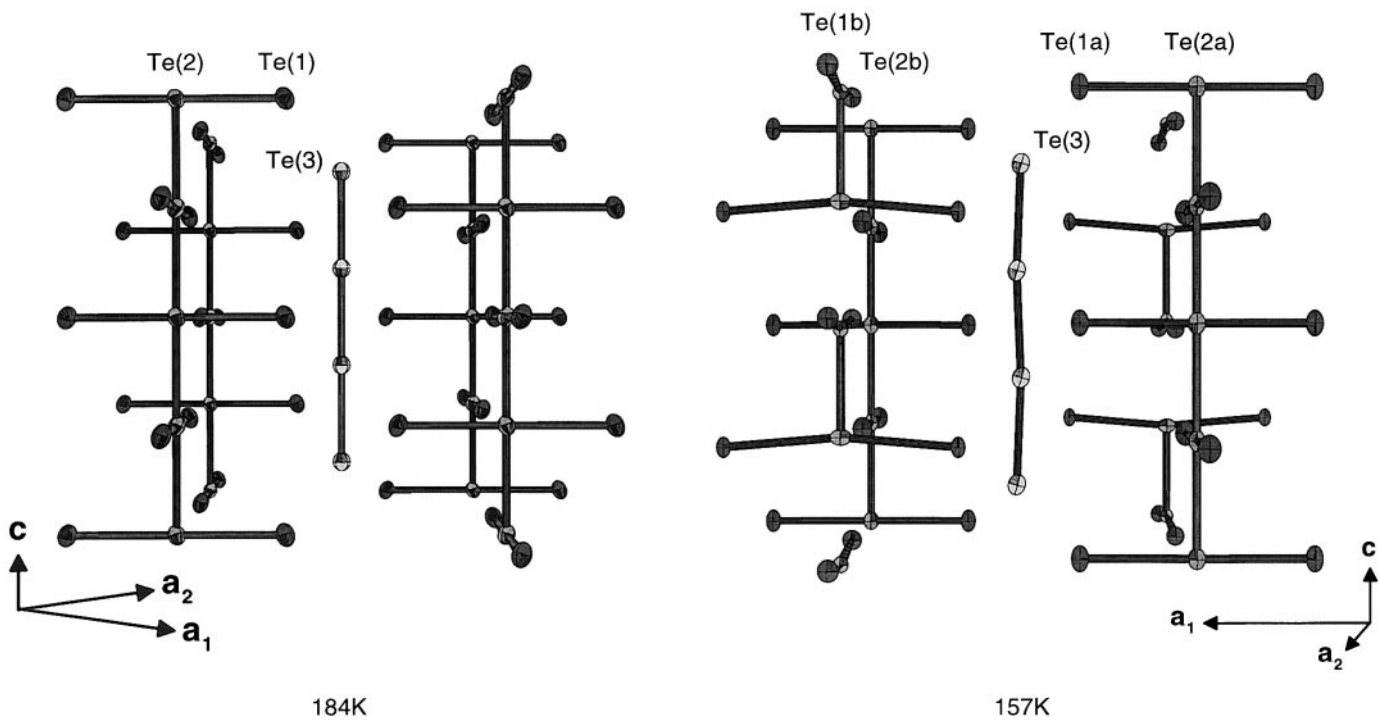

FIG. 9. Comparison of the Te framework of the different polymorphs of TlTe to illustrate the structural changes during transition.

a resistivity hump much smaller than 1 order of magnitude is experimentally observed at T_T (10). Further insights in the electronic structure of TlTe stem from band structure calculations, which will be discussed in detail in a subsequent contribution.

ACKNOWLEDGMENTS

We gratefully acknowledge the help of Dr. H.-G. Krane of the HASYLAB, Hamburg, for his assistance concerning the low-temperature investigations at the synchrotron beamline D3. HASYLAB at DESY is appreciated for the permission to use the synchrotron radiation facility. We also thank the Deutschen Forschungsgemeinschaft and the Fonds der Chemischen Industrie for financial support.

REFERENCES

1. H. Hahn and W. Klingler, *Z. Anorg. Allg. Chem.* **260,** 110 (1949).
2. T. Chattopadhyay, R. P. Santandrea, and H. G. von Schnering. *J. Phys. Chem. Solids* **46,** 351 (1985).
3. M. Chikashigé, *Z. Anorg. Allg. Chem.* **78,** 68 (1912).
4. A. P. Obukhov and N. S. Bubyreva, *Izvst. Sektora Fiz.-Khim. Anal.* **17,** 276 (1949).
5. M. Hansen, "Constitution of Binary Alloys." McGraw-Hill Book Co., New York, 1958.
6. A. Rabenau, A. Stegherr, and P. Eckerlin, *Z. Metalkunde* **51,** 295 (1960).
7. K. Burkhardt and K. Schubert, *J. Less-Common Metals* **18,** 426 (1969).
8. J. Weis, H. Schäfer, B. Eisenmann, and G. Schön, *Z. Naturforsch.* **29b**, 585 (1974).
9. A. A. Toure, G. Kra, R. Eholie, J. Olivier-Fourcade, and J.-C. Jumas, *J. Solid State Chem.* **87,** 229 (1990).
10. J. D. Jensen, J. R. Burke, D. W. Ernst, and R. S. Allgaier, *Phys. Rev. B* **6,** 319 (1972).
11. "SHELXTL PLUS, V.4.0, Program for Determination of Crystal Structures with X-Ray and Neutron Data." Siemens Analytical X-Ray Instruments. Inc., Madison WI, 1990.
12. K. Stöwe, *J. Solid State Chem.* **127,** 202 (1996).
13. R. Dronskowski and A. Simon, *Angew. Chem.* **101,** 775 (1989); *Angew. Chem., Int. Ed. Engl.* **28,** 758 (1989).
14. K. W. Hellmann, L. H. Gade, A. Steiner, D. Stalke, and F. Möller, *Angew. Chem.* **109,** 99 (1997).
15. S. Henkel, K. W. Klinkhammer, and W. Schwarz, *Angew. Chem.* **106,** 721 (1994); *Angew. Chem., Int. Ed. Engl.* **33,** 681 (1994).
16. N. Wiberg, K. Amelunxen, H. Nöth, M. Schmidt, and H. Schwenk, *Angew. Chem.* **108,** 110 (1996); *Angew. Chem., Int. Ed. Engl.* **35,** 65 (1996).
17. G. Treboux and J.-C. Barthelat, *J. Am. Chem. Soc.* **115,** 4870 (1993).
18. K. Stöwe, Ph.D. thesis, Erlangen, Germany, 1990.
19. K. Stöwe and H. P. Beck, *Z. Kristallogr.* **209,** 36 (1994).
20. e.g., "Unkonventionelle Wechselwirkungen in der Chemie metallischer Elemente" (B. Krebs, Ed.). VCH, Weinheim, 1992.
21. C. Janiak and R. Hoffmann, *J. Am. Chem. Soc.* **112,** 5924 (1990).
22. G. Llabres, O. Dideberg, and L. Dupont, *Acta Crystallogr. B* **28,** 2438 (1972).
23. K. Stöwe, *Z. Anorg. Allg. Chem.* **622,** 1423 (1996).
24. C. Adenis, V. Langer, and O. Lindqvist, *Acta Crystallogr. C* **45,** 941 (1989).